Article:

eprints@whiterose.ac.uk
https://eprints.whiterose.ac.uk/

A comparison study of InGaN/GaN multiple quantum wells grown on (111) silicon and (0001) sapphire substrates under identical conditions

To cite this article: C Zhu *et al* 2022 *J. Phys. D: Appl. Phys.* **55** 444003

View the article online for updates and enhancements.

A comparison study of InGaN/GaN multiple quantum wells grown on (111) silicon and (0001) sapphire substrates under identical conditions

C Zhu, C Xu, P Feng, X Chen, G M de Arriba, J Bai and T Wang*

Department of Electronic and Electrical Engineering, The University of Sheffield, Sheffield S1 3JD, United Kingdom

E-mail: t.wang@sheffield.ac.uk

CrossMark

Abstract

Due to an increasing demand of developing III-nitride optoelectronics on silicon substrates, it is necessary to compare the growth and optical properties of III-nitride optoelectronics such as InGaN based light emitting diodes (LEDs) on silicon substrates and widely used sapphire substrates. GaN-on-silicon suffers from tensile strain, while GaN-on-sapphire exhibits compressive strain. This paper presents a comparative study of InGaN/GaN multiple quantum wells (MQWs) grown on a silicon substrate and a sapphire substrate under identical conditions. It has been found that GaN strain status has a significant influence on the growth and the optical properties of InGaN/GaN MQWs. Photoluminescence measurements indicate the InGaN/GaN MQWs grown on a silicon substrate exhibit significantly longer wavelength emission than those on a sapphire substrate. Detailed x-ray diffraction measurements including reciprocal space mapping measurements confirm that both indium content and growth rate in the InGaN MQWs on the silicon substrate are enhanced due to the tensile strain of the GaN underneath compared with those on the sapphire substrate. This work also presents an investigation on strain evolution during the InGaN MQWs growth on the two different kinds of substrates. A qualitative study based on *in-situ* curvature measurements indicates that a strain change on the silicon substrate is much more sensitive to a growth temperature change than that on the sapphire substrate. It is worth highlighting that the results provide useful guidance for optimising growth conditions for III-nitrides optoelectronics on silicon substrates.

Keywords: InGaN/GaN quantum well, substrate, sapphire, silicon, strain

(Some figures may appear in colour only in the online journal)

* Author to whom any correspondence should be addressed.

J. Phys. D: Appl. Phys. **55** (2022) 444003

C Zhu *et al*

1. Introduction

It is ideal to employ a homo-epitaxial growth technique to obtain III–V compound semiconductors with high crystal quality, while hetero-epitaxy potentially generates lattice-mismatch induced strain, the most fundamental challenge which substantially complicates a growth mode and thus affect the optical properties of III–V semiconductors. Home epitaxy has been widely used in the growth of III–V compound semiconductors, leading to a great success in the fabrication of II–V semiconductor optoelectronics with high performance in the last few decades, in particular GaAs and InP based on optoelectronics for use in telecom applications [1–8]. However, the growth on III-nitride semiconductors are mainly based on lattice-mismatched hetero-epitaxy due to the lack of affordable native substrates. Sapphire and silicon are the two major substrates for the hetero-epitaxial growth of III-nitride semiconductors. The huge lattice-mismatch between either sapphire or silicon and GaN poses a great challenge in obtaining GaN with reasonably good crystal quality. GaN on sapphire suffers compressive strain due to the huge lattice mismatch of ∼16%, while GaN on silicon exhibits tensile strain as a result of the large difference in thermal expansion coefficient between GaN and Si (∼54%) in addition to the huge lattice mismatch between GaN and silicon (∼17%) [9–14]. It is well-known that the growth of GaN on either silicon or sapphire requires a high temperature of above 1000 °C. Such a high growth temperature makes the growth of GaN on silicon more challenging, as the large thermal expansion coefficient difference between GaN and Si makes GaN on silicon suffer tensile strain, thus leading to severe cracking issues [9–14]. Furthermore, due to the well-known melt-back issue (i.e. gallium can chemically react with silicon at a high temperature) [11–14], the classic two-step growth method which has led to a great success in growing GaN on sapphire cannot be applied in the growth of GaN on silicon. Therefore, a different approach, where an initial AlN buffer and then a strain engineering layer have to be utilised, has been developed to grow GaN on silicon, which further complicates the strain status of GaN on silicon. Any further device structures, such as InGaN/GaN multiple quantum wells (MQWs) normally acting as an active region are then grown.

It has been understood that stress modifies the vapour-solid thermodynamic equilibrium, reducing the solid-phase epitaxial composition towards lattice-matched conditions and thus limiting indium incorporation into GaN [15, 16]. In another word, an indium incorporation rate into GaN depends on the strain status of the GaN underneath. Normally, tensile stress enhances an indium incorporation rate into GaN, facilitating the growth of higher indium content in GaN which is crucial for achieving III-nitride emitters with a long emission wavelength such as green or yellow. This will help mitigate the well-known 'green/yellow gap' issues.

As mentioned above, GaN on sapphire is subjected to compressive strain. In contrast, GaN on silicon exhibit tensile strain. Therefore, it is expected that the InGaN MQWs grown on GaN-on-sapphire will be different from those grown on GaN-on-silicon even under identical growth conditions. In recent years, great progresses have been achieved on III-nitride optoelectronic devices on silicon substrates [17–19]. Especially, there is an increasing demand of developing microLED based microdisplays, where Si-CMOS is normally used as an electronic driver [9–14], which requires transferring the mature growth technologies for III-nitride emitters on GaN-on-sapphire to those on GaN-on-Si. However, so far, there is almost an absence in reporting a comparative study on the growth of InGaN MQWs on GaN-on-sapphire and GaN-on-silicon. This is the main purpose of our work presented in this paper.

2. Experimental

In this paper, both standard GaN-on-sapphire templates and standard GaN-on-Si templates were initially prepared by a standard metalorganic chemical vapour deposition (MOCVD) technique. Both templates were then loaded into a multiple wafer MOCVD chamber for further growth of InGaN/GaN MQWs simultaneously, meaning that the InGaN/GaN MQWs have been grown under identical conditions. An initial n-GaN layer was grown, followed by the growth of 30 pairs of $In_{0.05}Ga_{0.95}N$: 4.2 nm/GaN: 2.5 nm superlattice layers (SLs) as a pre-layer and then 5 periods of InGaN/GaN MQWs as an emitting region. Finally, a 20 nm p-AlGaN acting as an electron blocking layer and then a 200 nm p-GaN layer were grown. For simplicity, the sample grown on the GaN-on-Si template is denoted as Sample A, while the sample grown on the GaN-on-sapphire template is labelled as Sample B. In order to demonstrate reproducibility, such a comparative growth in the same growth run has been repeated by growing a second set of LEDs on a GaN-on-Si template and on a GaN-on-sapphire template, respectively.

Photoluminescence (PL) and detailed x-ray diffraction (XRD) measurements have been carried out on both samples, demonstrating a significant difference in both structure and optical properties. The InGaN/GaN MQWs on the GaN-on-sapphire exhibit an emission in the blue spectral region, while the InGaN/GaN MQWs on the GaN-on-silicon show a green emission. The detailed XRD measurements have confirmed that the indium content in the MQWs on the GaN-on-silicon is greater than its counterpart on the GaN-on-sapphire. It has also been found that the growth rate of the InGaN MQWs between the two samples is different.

Meanwhile, *in-situ* monitoring curvature measurements have been conducted, demonstrating that the sample on the GaN-on-Si exhibits significant tensile stress that is sensitive to a change in growth temperature, while the compressive stress that the sample on the GaN-on-sapphire exhibits is much less sensitive to a growth temperature variation. The stress for both samples has also been studied qualitatively. The results demonstrate that extra attention will have to be paid when the growth conditions which have been optimised for III-nitride optoelectronics on sapphire substrates are transferred to those on silicon substrates.
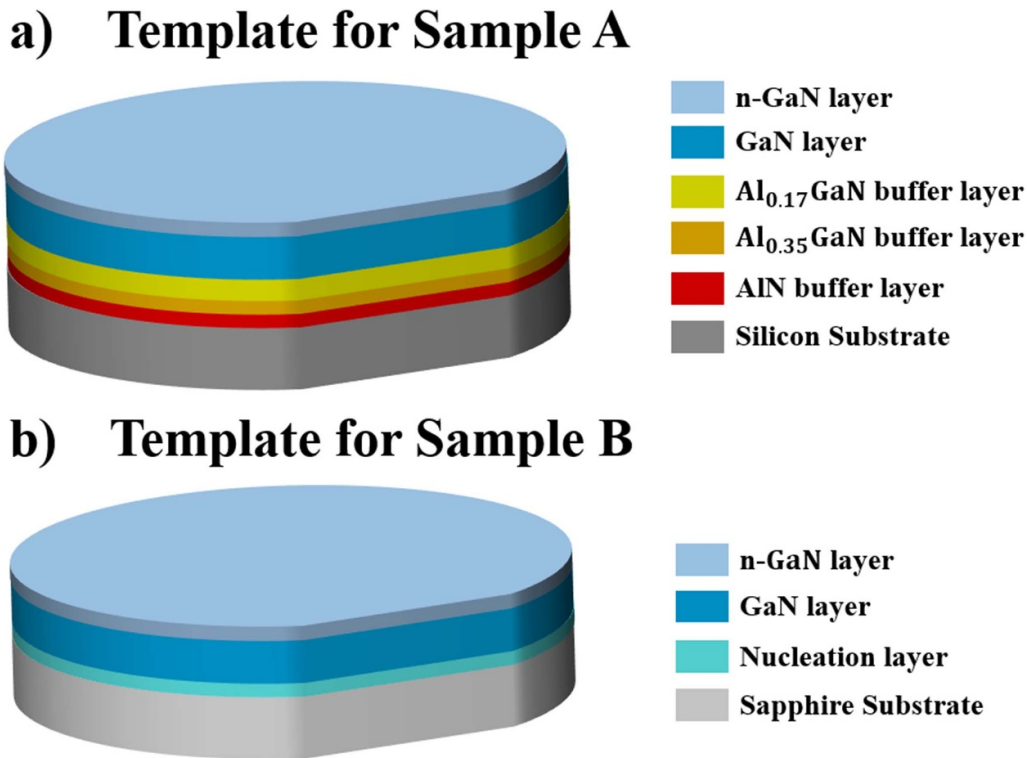
a) Template for Sample A

- n-GaN layer
- GaN layer
- $Al_{0.17}GaN$ buffer layer
- $Al_{0.35}GaN$ buffer layer
- AlN buffer layer
- Silicon Substrate

b) Template for Sample B

- n-GaN layer
- GaN layer
- Nucleation layer
- Sapphire Substrate

Figure 1. Schematic illustration of GaN-on-silicon template (a) and GaN-on-sapphire template (b).

3. Results and discussions

Two different kinds of GaN templates (i.e. GaN-on-sapphire templates and GaN-on-Si templates) have been prepared by a standard $3 \times 2''$ closed-coupled showerhead flip-top MOCVD system. For the GaN-on-sapphire templates, standard (0001) *c*-plane sapphire substrates were initially subjected to a high-temperature annealing process in H_2 ambience at 1150 °C, followed by the growth of a 25 nm thick low-temperature nucleation layer at 620 °C. Subsequently, the growth temperature was decreased to 1120 °C to carry out the growth of a nominally undoped GaN layer with a thickness of approximately 1.5 μm and finally a 300 nm silicon doped n-GaN layer. The GaN-on-Si templates were grown by using a step-graded AlN/AlGaN buffer approach to overcome a cracking issue which typically takes place during the cooling process [12–14, 20]. Standard (111) silicon substrates were initially annealed at 1350 °C for 10 min in H_2 ambience to thermally remove any native oxides. Subsequently, the temperature was reduced to 1000 °C and a trimethylaluminum pre-flow is then conducted without any NH_3 flowing for 40 s, followed by a thin low-temperature AlN layer and then a high-temperature AlN layer grown at 1290 °C. The total AlN thickness is around 200 nm. Afterwards, a 260 nm $Al_{0.35}Ga_{0.65}N$ layer and then a 440 nm $Al_{0.17}Ga_{0.83}N$ layer were grown as a step-graded AlGaN buffer, which aims to generate extra compressive strain to compensate for tensile strain which takes place during the cooling process after the subsequent growth of a thick GaN layer. A 1.5 μm GaN layer and then a 300 nm silicon doped

n-GaN were grown at 1120 °C. Figure 1 schematically illustrates these two kinds of GaN templates in detail.

Subsequently, the two templates were then reloaded into the multiple-wafer MOCVD chamber simultaneously for the further growth of a standard InGaN MQW LED structure in a same run under identical conditions. It is worth highlighting that the growth conditions which have been optimised for InGaN/GaN MQWs grown on sapphire but not on silicon have been chosen to use for such a comparative study.

PL measurements have been carried out using a 375 nm diode laser as an excitation source, which is directed by two aluminium mirrors with high reflectivity and then focused on a sample by an ultraviolet lens. The emission is introduced into a monochromator (Horiba SPEX 500M) by a pair of lenses and then detected by a thermoelectrically cooled charge-coupled device detector.

XRD measurements have been conducted by using a Bruker D8 x-ray diffractometer system, which is typically equipped with a copper (Cu) based anode generating the Cu Kα x-ray with a wavelength of 1.5418 Å. Along with a commercial Bruker RADS software for fitting and simulation, XRD measurements conducted in a ω-2θ scan mode have been used to determine the indium content and the layer thickness in the InGaN/GaN MQW region. Reciprocal space mapping (RSM) measurements have been carried out by performing an asymmetric scan along the (10–15) direction as usual [9, 21–27].
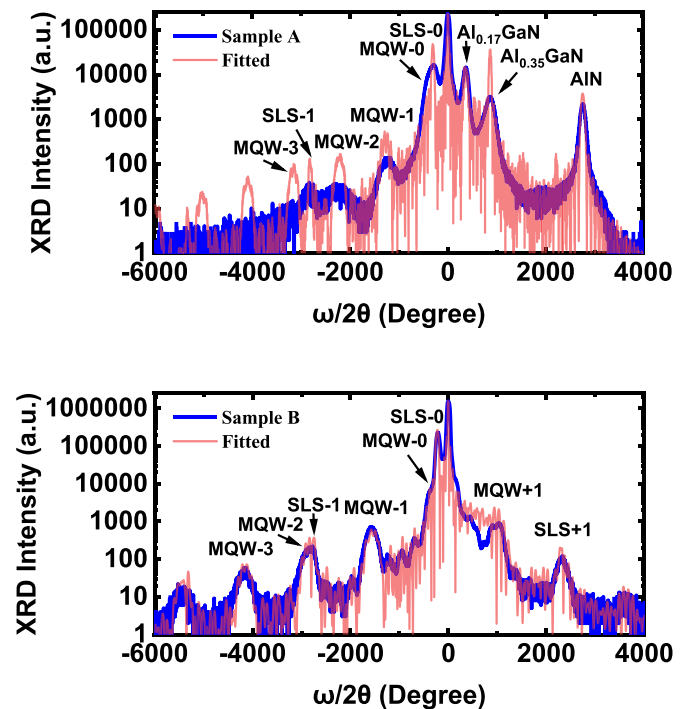
Figure 2 shows the PL spectra of both samples measured under identical conditions at room temperature, indicating that
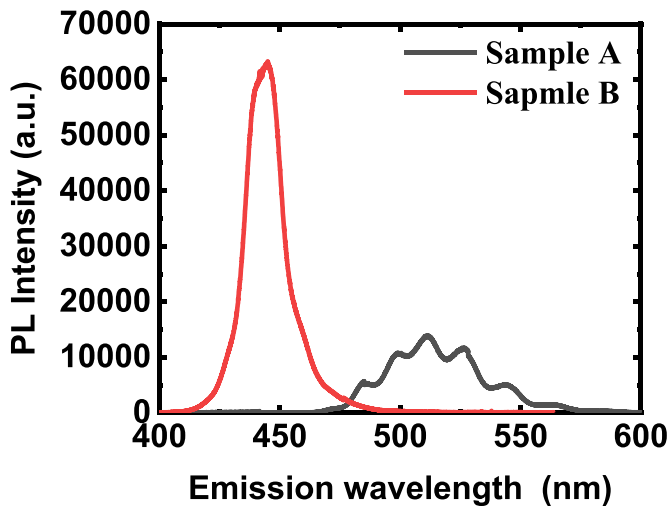
Figure 2. Photoluminescence spectra of Sample A and Sample B measured under identical conditions at room temperature.

Figure 3. XRD spectra measured in a ω-2θ scan mode for Sample A (a) and Sample B (b). In each case, the satellite peaks from the InGaN/GaN SLS as a standard pre-layer and the five periods of InGaN/GaN MQWs as an active region have been clearly observed. The detailed fitting has been obtained by using the commercial Bruker RADS software and considering the PL results and the results from our RSM measurements shown in figure 4.

Sample B exhibits a strong emission at 444 nm, while a green emission peak centred at 512 nm has been observed for Sample A. Furthermore, the emission peak from Sample B is much narrower than that from Sample A, while the emission intensity from Sample A is weaker than that from Sample B. As mentioned above, the growth conditions which were chosen for the growth of Sample A and Sample B simultaneously are optimised for InGaN/GaN MQWs grown on sapphire but *not on silicon*. Figure 2 clearly demonstrates that there exists a significant difference between Sample A and Sample B in terms of optical characterisation although their InGaN/GaN MQWs were grown in the same run under identical conditions. In order to make a further confirmation, PL measurements were performed on the second set of InGaN LEDs grown on a GaN-on-Si template and on a GaN-on-sapphire template, respectively, also showing very similar results, namely, the emission wavelength from the InGaN/GaN MQW sample grown on the GaN-on-sapphire template is much shorter than that on the GaN-on-Si template.

Figure 3 presents the XRD spectra of both Sample A and Sample B measured in a ω-2θ scan mode, where both the satellite peaks from the 30 pairs of the InGaN/GaN SLS and the 5 periods of InGaN/GaN MQWs have been clearly observed. These satellite peaks with different orders have also been marked. The indium composition, the InGaN quantum well thickness and the GaN barrier thickness of the InGaN/GaN MQWs in these two samples have been determined by combining the utilisation of the commercial Bruker RADS software for a simulation and the PL results. Table 1 lists the indium content, the InGaN quantum well thickness and the GaN barrier thickness for both Sample A and Sample B. Sample B shows the InGaN quantum wells with 13% indium content and a thickness of 2.3 nm and the GaN barriers with a thickness of 10.5 nm, while the indium content, and the InGaN quantum well thickness and the GaN barrier thickness of Sample A are 21%, 2.6 nm and 15.1 nm, respectively. Similar results have been obtained for the second set of samples. These
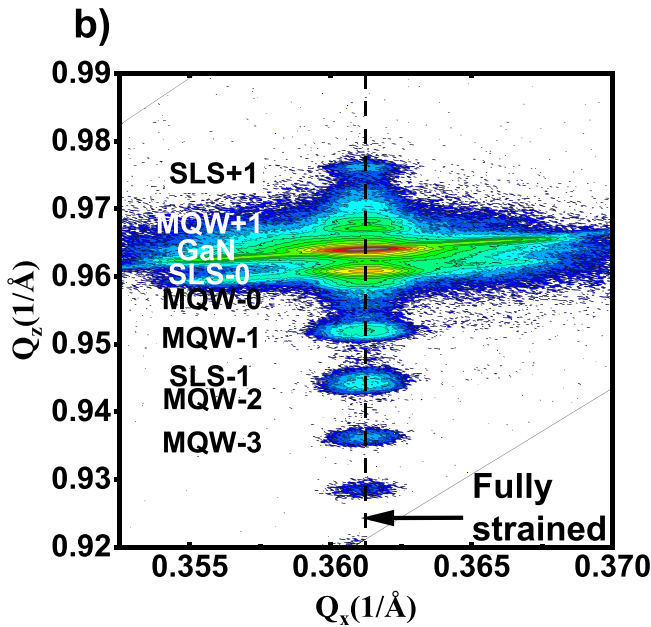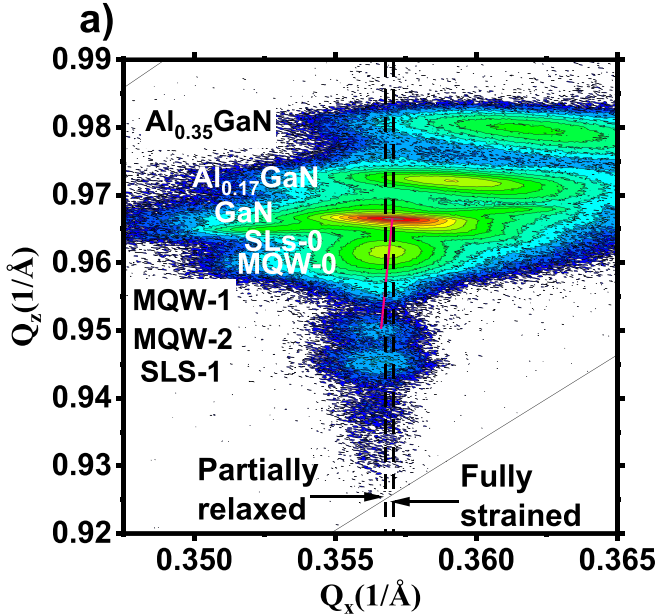
results mean that InGaN/GaN MQWs grown on a GaN-on-Si template exhibit higher indium content and a faster growth rate than that on a GaN-on-sapphire template. It has been reported that stress can change vapour-solid thermodynamic equilibrium, reducing the solid-phase epitaxial composition towards lattice-matched conditions and thus limiting indium incorporation into GaN [7, 12, 20, 28–30]. The higher indium content for InGaN/GaN MQWs on the GaN-on-Si template indicates that the tensile strain of the GaN underneath helps enhance the indium incorporation rate into GaN and the growth rate, due to the changes in thermodynamic limitations caused by strain differences in the template layers [31].

Please note that detailed RSM measurements have also been performed along the (10–15) orientation [9, 32] on both samples to determine the strain of the InGaN/GaN MQWs in both cases, one of the important parameters for our simulation to accurately determine the indium content and the InGaN quantum well thickness. Figure 4 shows the RSM results of Sample A and Sample B measured in an asymmetric diffraction scan along with the (10–15) orientation, demonstrating that the InGaN/GaN MQWs grown on the GaN-on-sapphire template are fully strained since all the satellite peaks from the InGaN/GaN MQW align with the vertical line which passes through the GaN peak, while it is not the case for Sample A. For the InGaN/GaN MQWs on the GaN-on-Si template (i.e. Sample A), a clear strain relaxation has been observed on the InGaN/GaN MQWs since the satellite peaks from the

J. Phys. D: Appl. Phys. **55** (2022) 444003

C Zhu *et al*

Table 1. Indium content in the InGaN QW; InGaN QW thickness and GaN barrier thickness determined from the XRD results and the PL results.
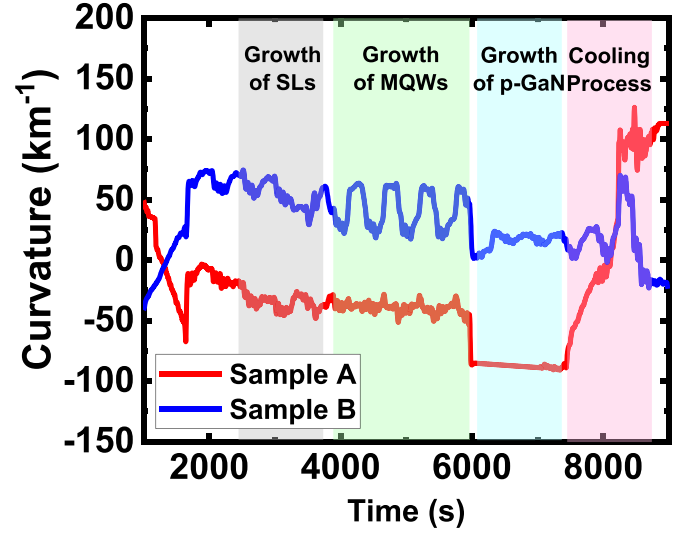
Sample no.	Emission wavelength (nm)	Indium Content (x)	InGaN well thickness (nm)	GaN barrier thickness (nm)
Sample A	512	0.21	2.6	15.1
Sample B	444	0.13	2.3	10.5

Figure 5. *In-situ* curvature measurements during the growth process for Sample A and Sample B.

Figure 4. RSM measured along the asymmetric (10–15) diffraction for Sample A (a) and Sample B (b).

InGaN/GaN MQWs inclines towards the relaxing direction. Detailed relaxation can be calculated by using equation (1) given below [21–27]:

$$R = \left(a_{\text{measured}}^{\text{InGaN}} - a_{\text{measured}}^{\text{GaN}} \right) / \left(a_{\text{reference}}^{\text{InGaN}} - a_{\text{reference}}^{\text{GaN}} \right) \quad (1)$$

where $a_{\text{measured}}^{\text{InGaN}}$ and $a_{\text{measured}}^{\text{GaN}}$ are the measured in-plane lattice constants, respectively; and $a_{\text{reference}}^{\text{InGaN}}$ and $a_{\text{reference}}^{\text{GaN}}$ are the in-plane lattice constants in a fully relaxed situation, respectively.

Based on equation (1) and the RSM results, 5% relaxation has been determined for Sample A and this figure has been used for our XRD simulation/fitting discussed above.

The strain evolution of Sample A and Sample B during the growth process has been investigated by using a commercial Laytec EpiCurve TT system which is equipped with the MOCVD system. Two parallel laser beams with a wavelength of 635 nm are introduced into a measured wafer through the optical port of the MOCVD and are then reflected back through the optical port. The curvature of the wafer can be determined from the distance between the two reflected laser beams. Figure 5 shows the results of the *in-situ* curvature measurements during the growth of Sample A and Sample B. A positive value indicates that a wafer is in a concave shape, meaning that the wafer is under tensile stress, while a negative value represents a convex shape meaning that the wafer is under compressive stress. Figure 5 shows that Sample A exhibits positive curvature values before and after the growth process, indicating that the GaN on the silicon substrate is under tensile stress at room temperature. In contrast, Sample B exhibits a little bit convex shape, which indicates that the GaN on the sapphire substrate is under compressive stress at room temperature. Furthermore, during the growth process of the InGaN/GaN MQW, Sample B is constantly under compressive stress, while Sample A experiences a variation in tensile

J. Phys. D: Appl. Phys. **55** (2022) 444003

C Zhu *et al*

stress which is due to a growth temperature change between the InGaN quantum wells and the GaN barriers. This means that the strain variation that occurred to Sample B is much less sensitive to a growth temperature change compared to Sample A.

The Stoney formula given below [33, 34] is further used to estimate stress (labelled as σ) of the GaN on silicon or sapphire and the stress of Sample A and Sample B after the InGaN MQWs growth,

$$\sigma = \frac{\kappa E_s t_s^2}{6 t_f (1 - \vartheta_s)} \qquad (2)$$

where t_f and t_s represent the thickness of a film on a substrate and the thickness of the substrate, respectively; E_s and ϑ_s are Young's modulus; and the Poisson's ratio, respectively. The thicknesses t_s of the silicon substrate and the sapphire substrates are 430 μm and 330 μm, respectively, which are about 100 times thicker than the thickness of the epilayer of either Sample A or Sample B. Based on equation (2), the stress that the GaN layers of Sample A and Sample B suffer is -0.34 GPa and 0.35 GPa, respectively. Their stress during the growth of InGaN/GaN MQWs for Sample A and Sample B is -0.35 GPa and 0.17 GPa, respectively.

The thermal stress (labelled as σ_{th}), which are generated during a cooling process, can be estimated by equation (3) provided below [32, 35],

$$\sigma_{th} = \frac{E_{film}}{1 - v_{film}} (\alpha_1 - \alpha_2)(T_1 - T_2) \qquad (3)$$

where T_1 and T_2 are the growth temperature and room temperature, respectively; α_1 and α_2 are the thermal expansion coefficients of the substrate and the epilayer, respectively. E_{film} *and* v_{film} are Young's modulus and the Poisson ratio of the epilayer, respectively. Based on equation (3), the thermal stress of Sample A and Sample B is -0.78 GPa and 0.55 GPa, respectively, which are consistent with the stress obtained from the *in-situ* curvature measurements.

4. Conclusion

In summary, a systematic study on the influence of different substrates on the growth and the optical properties of InGaN/GaN MQWs has been carried out by simultaneously growing InGaN/GaN MQWs on a GaN-on-Si template and a GaN-on-sapphire template in a same growth run. Our results demonstrate a major difference between them. The MQWs grown on the GaN-on-Si template shows significantly longer wavelength emission than those on the GaN-on-sapphire template. Detailed XRD measurements confirm that the MQWs grown on the GaN-on-Si template exhibit an enhancement in both indium content and growth rate than those on the GaN-on-sapphire. These major differences can be attributed to the changes in thermodynamic limitations, caused by the tensile strain that the GaN-on-Si suffers. *In-situ* curvature measurements during the MQWs growth suggest that more attention will have to be paid to a temperature change during growth

on the GaN-on-Si template than on the GaN-on-sapphire template, as the strain for the growth on the GaN-on-Si template is much more sensitive to a temperature change compared to the GaN-on-sapphire case.

Data availability statement

The data that support the findings of this study are available upon reasonable request from the authors.

ORCID iDs

J Bai ⓘ https://orcid.org/0000-0002-6953-4698
T Wang ⓘ https://orcid.org/0000-0001-5976-4994

References

[1] Avramescu A, Lermer T, Müller J, Eichler C, Bruederl G, Sabathil M, Lutgen S and Strauss U 2010 *Appl. Phys. Express* **3** 061003
[2] Oh M-S, Kwon M-K, Park I-K, Baek S-H, Park S-J, Lee S and Jung J 2006 *J. Cryst. Growth* **289** 107–12
[3] Funato M, Ueda M, Kawakami Y, Narukawa Y, Kosugi T, Takahashi M and Mukai T 2006 *Jpn. J. Appl. Phys.* **45** L659
[4] Hang S J, Lai W C, Su Y K, Chen J F, Liu C H and Liaw U 2002 *IEEE J. Sel. Top. Quantum Electron.* **8** 278–83
[5] Ngo T H, Gil B, Valvin P, Damilano B, Lekhal K and De Mierry P 2015 *Appl. Phys. Lett.* **107** 122103
[6] Barletta P T, Acar Berkman E, Moody B F, El-Masry N A, Emara A M, Reed M J and Bedair S 2007 *Appl. Phys. Lett.* **90** 151109
[7] Wang T 2016 *Semicond. Sci. Technol.* **31** 093003
[8] Dussaigne A *et al* 2020 *J. Appl. Phys.* **128** 135704
[9] Amani E, Khojier K and Zoriasatain S 2018 *Appl. Phys.* A **124** 1–8
[10] Liu J-L *et al* 2015 *Chin. Phys.* B **24** 067804
[11] Dolmanan S B, Teo S L, Lin V K, Hui H K, Dadgar A, Krost A and Tripathy S 2011 *Electrochem. Solid-State Lett.* **14** H460
[12] Pereira S, Correia M, Pereira E, O'Donnell K, Alves E, Sequeira A, Franco N, Watson I and Deatcher C 2002 *Appl. Phys. Lett.* **80** 3913–5
[13] Dadgar A, Hums C, Diez A, Bläsing J and Krost A 2006 *J. Cryst. Growth* **297** 279–82
[14] Cai Y, Zhu C, Jiu L, Gong Y, Yu X, Bai J, Esendag V and Wang T 2018 *Materials* **11** 1968
[15] Aumer M, LeBoeuf S, Bedair S, Smith M, Lin J and Jiang H 2000 *Appl. Phys. Lett.* **77** 821–3
[16] Iida D, Zhuang Z, Kirilenko P, Velazquez-rizo M, Najmi M A and Ohkawa K 2020 *Appl. Phys. Lett.* **116** 162101
[17] Park J-S, Tang M, Chen S and Liu H 2020 *Crystals* **10** 1163
[18] Hsu L-H *et al* 2021 *Micromachines* **12** 1159
[19] Feng M, Liu J, Sun Q and Yang H 2021 *Prog. Quantum Electron.* **77** 100323
[20] Tawfik W Z, Song J, Lee J J, Ha J S, Ryu S-W, Choi H S, Ryu B and Lee J K 2013 *Appl. Surf. Sci.* **283** 727–31

[21] Schuster M, Gervais P, Jobst B, Hösler W, Averbeck R, Riechert H, Iberl A and Stömmer R 1999 *J. Phys. D: Appl. Phys.* **32** A56

[22] Young E C, Romanov A E and Speck J S 2011 *Appl. Phys. Express* **4** 061001

[23] Wright A 1997 *J. Appl. Phys.* **82** 2833–9

[24] Moram M and Vickers M 2009 *Rep. Prog. Phys.* **72** 036502

[25] Ley R, Chan L, Shapturenka P, Wong M, DenBaars S and Gordon M 2019 *Opt. Express* **27** 30081–9

[26] Detchprohm T, Hiramatsu K, Itoh K I K and Akasaki I A I 1992 *Jpn. J. Appl. Phys.* **31** L1454

[27] Paszkowicz W 1999 *Powder Diffr.* **14** 258–60

[28] Inatomi Y, Kangawa Y, Ito T, Suski T, Kumagai Y, Kakimoto K and Koukitu A 2017 *Jpn. J. Appl. Phys.* **56** 078003

[29] Shimizu M, Kawaguchi Y, Hiramatsu K and Sawaki N 1997 *Jpn. J. Appl. Phys.* **36** 3381

[30] Sonderegger S, Feltin E, Merano M, Crottini A, Carlin J F, Sachot R, Deveaud B, Grandjean N and Ganière J D 2006 *Appl. Phys. Lett.* **89** 232109

[31] Johnson M C, Bourret-Courchesne E D, Wu J, Liliental-Weber Z, Zakharov D, Jorgenson R, Ng T, McCready D E and Williams J R 2004 *J. Appl. Phys.* **96** 1381–6

[32] Zhou S, Vantomme A, Zhang B, Yang H and Wu M F 2005 *Appl. Phys. Lett.* **86** 081912

[33] Feng X, Huang Y and Rosakis A 2007 *J. Appl. Mech.* **74** 1276

[34] Janssen G 2007 *Thin Solid Films* **515** 6654–64

[35] Ahmad I, Holtz M, Faleev N and Temkin H 2004 *J. Appl. Phys.* **95** 1692–7